RESILIENT INFRASTRUCTURE
June 1–4, 2016

DECENTRALIZED SEMI-ACTIVE CONTROL FOR MULTI-PERFORMANCE-BASED DESIGN

YJ Cha
Assistant Professor, University of Manitoba, Canada.

ABSTRACT

Traditional performance-based design (PBD) that has a single performance level has been widely researched by changing section sizes of structural members or material properties to resist single hazard levels. However, this approach has limitations in terms of achieving performance and alternative design options for the owner. To overcome these limitations of the traditional PBD method, a multi-performance-based control design (MPBCD) methodology is newly proposed. The MPBCD integrates a decentralized semi-active control algorithm with semi-active smart damping devices and an advanced multi-objective optimization method. The multi-objective optimization is used to achieve various sets of performance-based control designs. The control designs satisfy multiple performance levels under multiple hazard levels without changing cross-section sizes or material properties of structural members. This MPBCD provides multiple sets of control designs (i.e., control device layouts with control design variables) to minimize design costs and maximize control effectiveness. The multiple sets of designs offer optimal performance-based control design covering a broad range of hazard levels with various performance levels. This numerical study uses an advanced decentralized semi-active controller and large-scale 200-kN magnetorheological (MR) dampers installed in a nine-story moment-resisting frame (MRF) building. From the multi-objective optimization technique, multiple layouts of control devices and controller parameters for multiple performance levels under multiple hazard levels are investigated.

Keywords: multi-performance-based design; semi-active control; magnetorheological damper; multi-objective genetic algorithm; nonlinear model; nonlinear time-history analysis

1. INTRODUCTION

Traditional performance-based design methods have been forced on the optimization of cross-sectional areas of structural members or material properties to satisfy a predefined single objective under a single hazard level. For example, Moehle (1992) proposed a force-based design method by calculation of ductility capacity and it was extended to displacement-based design. Fujitani et al. (2005) proposed a new method for performance-based design to address earthquake loads by considering the concept of cost-performance. Lagaros et al. (2006) carried out optimization using an evolutionary algorithm to minimize total structure weight and maximize interstory drift of the structure subjected to seismic load. Priestley et al. (2007) proposed a displacement-based performance-based design method which uses an equivalent liner single-degree-of-freedom (SDOF) to account for multi DOF. However, the above-mentioned studies were limited to focusing on the optimization of structural member sizes for performance-based design, which means that these approaches are not able to implement to existing structures.

As an another approach to reducing the seismic responses of civil structures, many control algorithms have been developed, such as clipped-optimal controllers (COC) by Dyke et al. (1996), a modified modulated homogeneous friction controller by He et al. (2003), resetting a semi-active stiffness damper by Yang et al. (2000) and Yang and Agrawal (2002), turbo-Lyapunov control by Cha and Agrawal (2013a), and decentralized output feedback polynomial control (DOFPC) by Cha and Agrawal (2013b). Moreover, advanced wavelet based controllers have been also developed by El-Khoury and Adeli (2013). These theoretical and technical achievements in structural control enable civil engineers to apply control strategies to performance-based designs. For example, a simplified design procedure and performance-based seismic design for a preliminary frame structure was proposed using high-damping elastomeric materials by Lee et al. (2005, 2009). A performance-based design using a semi-active control strategy for use with variable hydraulic dampers was proposed by Kurata et al. (2002). Hejazi et al. (2013) carried out optimization of viscous damper layouts to reduce structural responses about single earthquakes for three-dimensional structures. However, the simplified procedure for performance-based design requires iterative studies to find design parameters that meet performance objectives. The simplified control device mechanical models used in previous studies have deficiencies when capturing highly nonlinear hysteretic behavior based on time-varying control signals subjected to time-history ground motions. Also, these performance-based design methods still need engineering judgment and trial-and-error based iterations to determine the locations and numbers of control devices at each story of the building. The feasible domains to install control devices for high-rise buildings are too large to get meaningful solutions based on trial-and-error approaches (Cha et al., 2012, 2013a, 2013b). Furthermore, all of the proposed approaches above were focused on a single performance target under a single hazard level. These limitations may not offer enough information to determine eventual performance levels under specific hazard levels when the owner has a limited budget.

2. CONCEPT AND OBJECTIVES OF NEW MULTI-PERFORMANCE-BASED CONTROL DESIGN

A new performance-based control design method is proposed in this paper to overcome traditional performance-based design approaches. A multi-performance-based design approach is required to explore all conflicting design objectives (i.e., efficiency and cost) in a Pareto-optimal sense. Therefore, this paper proposes a new methodology for multi-performance-based control design (MPBCD) using semi-active control and multi-objective optimization to provide all possible design sets, satisfying multiple performance levels (PLs) subjected to multiple hazard levels (HLs) with a single trial of optimization using parallel computing. The MPBCD uses decentralized semi-active control algorithms and layouts of control devices for each story of a structure instead of changing structural member cross-section sizes to reduce seismic responses and eventually satisfy PLs under HLs. A nine-story steel moment-resisting frame (MRF) building is used as an example. The results are validated by carrying out nonlinear dynamic time-history analyses (NLDTHA) using a set of earthquake ground motions.

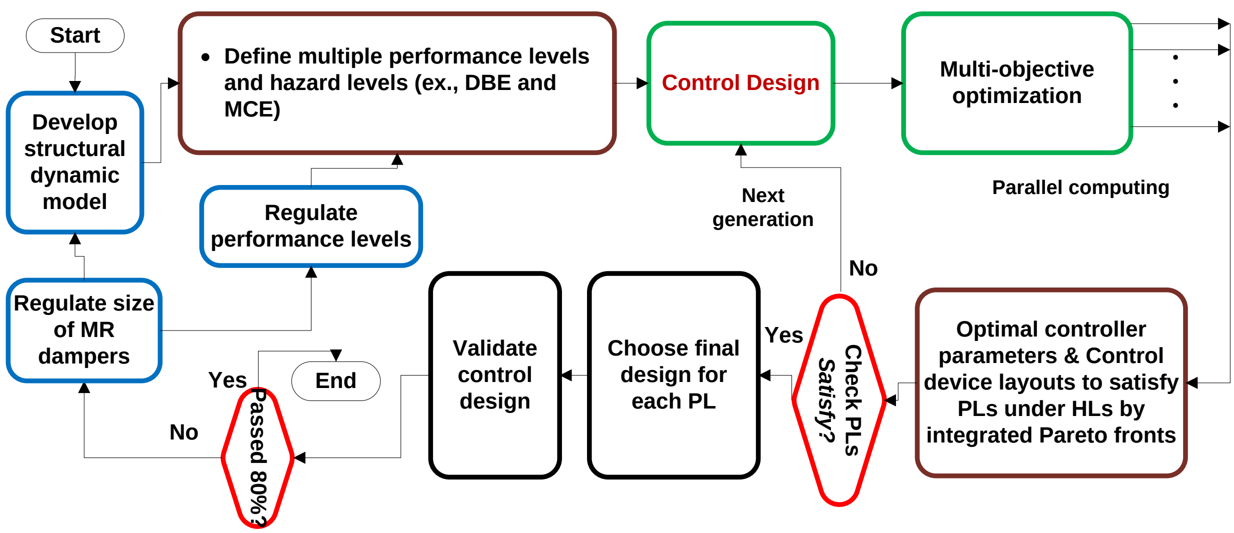

Figure 1: Procedure for multi-performance-based control design using multi-objective optimization

The details of the new MPBCD methodology by combining a control approach and multi-objective genetic algorithms (MOGAs) are shown in Figure 1. The first step of the MPBCD procedure is developing a numerical model including control design of a structure using a finite element method that considers material nonlinearity. The second step is defining design objectives in which multiple performance levels and hazard levels are determined based on the spectral response acceleration parameters obtained from the hazard maps. The third step is to design a controller. The fourth step involves the multi-objective optimizations of the design variables for the controller and control device layouts. In this step, the control design variables and control device layouts are simultaneously explored within a Pareto-optimal solution set for the predefined HLs to satisfy predefined PLs. If the performance levels are achieved, the MOGA process is stopped; otherwise, the optimization process will be continued. The sixth step is choosing the proper control design device layouts for each performance level subjected to each hazard level. As a final step, nonlinear dynamic time-history analyses (NLDTHA) are carried out using 20 to validate the design solutions for each MPBCD case. If the validation failed using the suite of earthquakes, the optimization procedure goes back to the first step to redefine the size of the control device and regulate performance levels.

3. SEMI-ACTIVE CONTROL STRATEGY AND MR DAMPERS

As an semi-active controller, a decentralized output feedback polynomial controller (DOFPC) was chosen (Cha & Agrawal 2013d). The control voltage of the DOFPC is determined by two third-order polynomial equations representing a relationship with interstory drift and velocity across control devices. 200-kN magnetorheological (MR) dampers are selected as the semi-active control devices. A phenomenological damper model (Spencer et al., 1997) was chosen.

4. STRUCTURE MODEL

A nine-story benchmark structure designed for Los Angeles, California, for structural control studies under the SAC Phase II Steel Project at the American Society of Civil Engineers (ASCE) is used for example numerical studies (Ohtori et al., 2004). This building is composed of 45.73 m by 45.73 m in plan and 37.19 m in total elevation with moment resisting frames in both N-S and E-W directions. The numerical model of the structure was developed using MATLAB (2007). To account for material nonlinearities, a bilinear hysteresis model is used to characterize the nonlinear bending stiffness of the structural members during strong earthquakes. The incremental governing equations of motion for the nonlinear structural system take the following form based on the Newmark-β time-step integration method. Reduced-order state space equations are established as

[1] $$\dot{\mathbf{x}}_{k+1}^{d} = \mathbf{A}_k^d \mathbf{x}_k^d + \mathbf{B}_k^d \mathbf{F}_k^d + \mathbf{E}^d \ddot{x}_g$$

[2] $$\mathbf{y}_m = \mathbf{C}_m \mathbf{x} + \mathbf{D}_m \mathbf{F} + \mathbf{F}_m \ddot{x}_g + \mathbf{v}$$

[3] $$\mathbf{y}_k^{ed} = \mathbf{C}_k^{ed} \mathbf{x}_k^{ed} + \mathbf{D}_k^{ed} \mathbf{F}_k^{ed} + \mathbf{E}^{ed} \ddot{x}_g$$

where $\mathbf{F}_k^d = \begin{bmatrix} f_k^1 & f_k^2 & \mathbf{L} & f_k^n \end{bmatrix}^T$; f_k^n is the *i*th floor MR damper; n is the number of the story; and $\mathbf{A}_k^d$, $\mathbf{B}_k^d$, $\mathbf{E}^{md}$, $\mathbf{C}_k^{md}$, $\mathbf{D}_k^{md}$, $\mathbf{F}_k^{md}$, $\mathbf{C}_k^{ed}$, $\mathbf{D}_k^{ed}$, and $\mathbf{E}^{ed}$ are reduced-order coefficient matrices. Also, $\mathbf{x}$ is the design-state vector, and $\mathbf{y}_k^{ed}$ and $\mathbf{y}_k^{md}$ are vectors of evaluated and measured responses, respectively.

5. MULTI-OBJECTIVE GENETIC ALGORITHMS

The performance-based control design problem includes an accumulated high-order complex nonlinear problem due to high nonlinear behavior of the control device, locations and numbers of control devices, and variables of control algorithms. The control algorithm accounts for nonlinear control signals to satisfy multiple performance objectives under nonlinear ground motions. To counter these high nonlinearities in optimization problems, a multi-objective gene manipulation genetic algorithm (Cha et al., 2013b) is implemented. A gene manipulation genetic algorithm (GMGA) (Cha et al., 2013b) uses dynamic encoding genotype/phenotype implicit redundant representation (IRR) genetic algorithms (GAs) (Raich & Ghaboussi, 2000) for encoding policies to address the complex high-order nonlinear optimization problem, and it uses non-dominated sorting genetic algorithms-II (NSGA-II) (Deb et al., 2000) for the non-dominated sorting and multi-objective selection method. To get a better child population, a predefined portion of the current parent population is used for the gene manipulation process to create a more competitive child for the next generation when compared to traditional NSGA-II. This advanced multi-objective optimization method showed robust performance to find Pareto-optimal solutions within large complex problem domain through many case studies (Cha et al., 2013b; Cha and Buyukozturk 2015). Many derivative-free optimization methods such as particle swarm optimizations and Pareto archived evolution strategies are available to carry out this optimization.

6. PERFORMANCE AND HAZARD LEVELS

All buildings in civil structures are classified into three seismic use groups according to the intended occupancy, objectives of usage, and damage consequences from the ASCE building code. The three seismic hazard levels are defined and can be distinguished by return period and probability of exceedance. A building's performance is classified into seven different performance levels depending on the maximum interstory drift in the entire building, as shown in Table 1 (FEMA, 2000a, 2000b; Ganzerli et al., 2000; Ghobarah, 2001). The seven performance levels are 1) no damage state; 2) operational (OP); 3) slight damage state, immediate occupancy (IO); 4) light damage state, damage control (DC); 5) moderate damage state, life safety (LS); 6) heavy damage state, collapse prevention (CP); and 7) collapsed state.

Table 1: Performance levels, damage states, and maximum interstory drifts

Performance level	Damage state	Maximum interstory drift (%)
1	None	Δ <0.2
2: (Operational: OP)	Slight	0.2< Δ <0.5
3: (Immediate Occupancy: IO)	Light	0.5< Δ <0.7
4: (Damage Control: DC)	Moderate	0.7< Δ <1.5
5: (Life Safety: LS)	Heavy	1.5< Δ <2.5
6: (Collapse Prevention: CP)	Major	2.5< Δ <5.0
7	Collapsed	5.0< Δ

(): FEMA (2000b) structural performance levels

Two different hazard levels are used for the nine-story building structure. The first hazard level is the maximum considered earthquake (MCE) ground motion; its two-thirds intensity of the MCE ground motion is used as a design-based earthquake (DBE). The MCE is represented by response spectra that have a 2% probability of exceedance in 50 years (FEMA, 2003). For each hazard level, two different performance levels are also defined. The performance levels defined as PL1, PL2, PL3, and PL4, respectively. The details of PLs and HLs are presented in Table 2.

Table 2: Objective performance levels and hazard levels

Performance level	Maximum interstory drift (%)	Hazard level
PL1: IO	0.7	DBE
PL2: DC	1.0	DBE
PL3: DC	1.3	MCE
PL4: LS	1.7	MCE

Two objective functions are formulated to maximize the control efficiency and minimize control cost in order to achieve the four performance levels subjected to two hazard levels. The first objective is maximum interstory drift in the entire structure subjected to an earthquake. The second objective is total number of MR dampers installed in the entire structure. These two objectives represent the efficiency and cost of the semi-active control to reduce structure responses.

7. SIMULATION RESULTS

The hazard levels should be determined to evaluate the effect of uncertainty in earthquake ground motions on structural responses. The response acceleration parameters can be obtained from ground hazard maps distributed with guidelines in case the hazard level corresponds to one in the ground-shaking hazard maps. In this paper, the building is located in the state of California, and the acceleration parameters are obtained from the maps (FEMA, 2003). These acceleration parameters should be modified to account for site class effects and then used to construct the design spectrum. For the specific location of the building, spectral acceleration parameters S_s (short period spectral acceleration) and S_1 (1 second period spectral acceleration) are 1.0, and 0.4, respectively. Site class effect parameters F_a and F_v are 1.0 because of assumed site class B from FEMA 450. To find Pareto-optimal control design layouts, the El Centro earthquake is chosen as an objective earthquake and scaled to the design spectrum. The spectral acceleration at T_n (i.e, 2.25) of the objective earthquake is 0.1222g.

Table 3: Possible MR damper layout sets for performance levels 0.7% and 1.0% under DBE

Floor	1st	2nd	3rd	4th	5th	6th	7th	8th	9th	Total
%	Performance level 0.7% under DBE									
0.606	8	8	8	8	8	8	8	8	6	70
0.612	8	8	8	8	8	6	8	8	6	68
0.618	8	8	8	8	8	6	8	8	4	66
⋮	⋮	⋮	⋮	⋮	⋮	⋮	⋮	⋮	⋮	⋮
0.682	8	8	2	8	6	2	8	8	2	52
0.694	***8***	***6***	***2***	***8***	***6***	***2***	***8***	***8***	***2***	***50***
Performance level 1.0% under DBE										
0.710	8	8	2	6	4	4	8	8	0	48
0.725	8	2	4	8	6	0	8	8	2	46
0.737	8	0	4	8	6	0	8	8	2	44
⋮	⋮	⋮	⋮	⋮	⋮	⋮	⋮	⋮	⋮	⋮
0.996	***6***	***0***	***0***	***0***	***0***	***0***	***4***	***8***	***0***	***18***
1.022	6	0	0	0	0	0	4	6	0	16
1.045	6	0	0	0	0	0	4	4	0	14
1.077	2	0	0	0	0	0	4	6	0	12
1.105	2	0	0	0	0	0	0	8	0	10

Table 4: Possible MR damper layout sets for performance levels 1.3% and 1.7% under MCE

Floor	1st	2nd	3rd	4th	5th	6th	7th	8th	9th	Total
%	Performance level 1.3% under MCE									
1.093	8	8	8	8	8	8	8	8	6	70
1.102	8	8	8	8	8	6	8	8	6	68
1.110	8	8	8	8	8	4	8	8	6	66
⋮	⋮	⋮	⋮	⋮	⋮	⋮	⋮	⋮	⋮	⋮
1.306	***8***	***8***	***6***	***8***	***0***	***0***	***0***	***8***	***4***	***42***
%	Performance level 1.7% under MCE									
1.339	8	8	4	8	0	0	0	8	4	40
1.372	8	8	4	6	0	0	2	8	2	38
1.406	8	8	6	4	0	0	0	8	2	36
⋮	⋮	⋮	⋮	⋮	⋮	⋮	⋮	⋮	⋮	⋮
1.694	***8***	***2***	***4***	***0***	***0***	***0***	***0***	***8***	***0***	***22***

MOGA and nonlinear time-history analysis are integrated to explore near-optimal sets of Pareto-optimal control device layouts and controller variables at each story. GMGA is implemented to account for high nonlinear dynamic characteristic behaviors of MR dampers and the control algorithm and those complex relationships between optimal damper layouts and control signals under earthquake ground motions. Each solution on each Pareto-optimal front provides a unique MR damper layout and design variables of a semi-active controller for each story in which the solution can be considered as a candidate of the performance-based control design. The results indicate that increasing the number of MR dampers has a beneficial effect on reducing drift, up to a total of approximately 70 MR dampers, which are installed to obtain maximum interstory drift at about 0.606% under DBE and about 1.093% under MCE. The reduction from 1.46% (i.e., uncontrolled maximum interstory response) to 0.606% (i.e., controlled maximum interstory response by DOFPC) under DBE and the reduction from 2.09% (i.e., uncontrolled maximum interstory response) to 1.093% (i.e., controlled maximum interstory response by DOFPC) under MCE are significantly remarkable without changing the structural member types, sizes, or material prosperities.

Each of the Pareto-optimal fronts from the DOFPC contains almost 30 sets of MR damper layouts, and each layout design identifies a different trade-off between maximum drift as control efficiency and control cost. For the DBE hazard level, the sets found can be used for the PL1, PL2, PL3, and PL4 under DBE and MCE hazard levels, respectively, as presented in Tables 3 and 4. Engineers can use this information to choose an appropriate design that best meets their performance levels and hazard levels by considering available budget and their environmental and structural limitations to designing control device layouts and controllers.

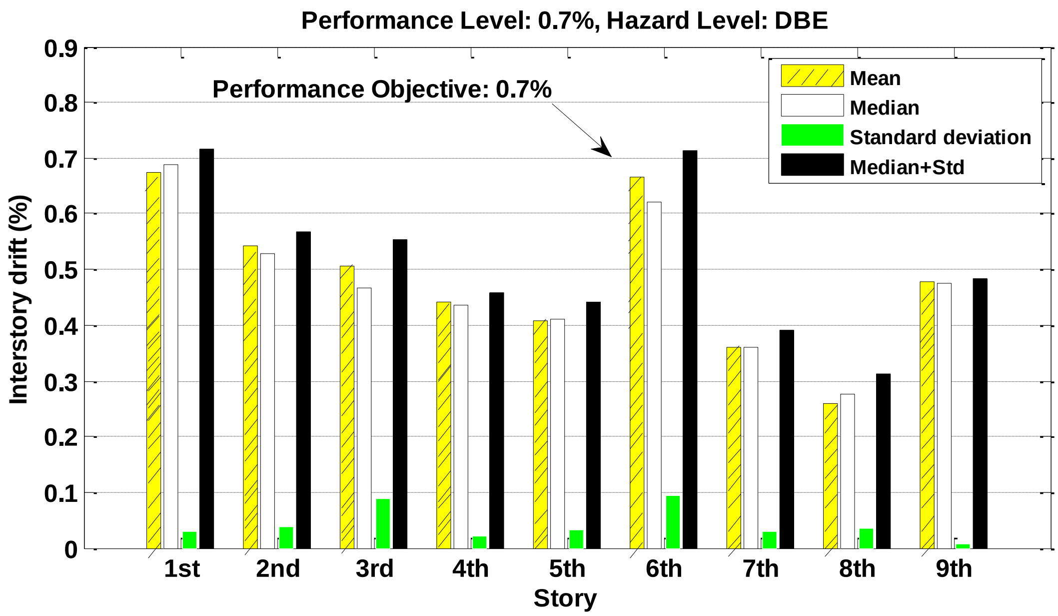

Figure 2: Statistical comparison of interstory drifts for the 0.7% PL under DBE HL

Four bold and italic MR damper design layouts are selected from Tables 3 and 4 in terms of minimal control cost with best efficiency and these layouts are used to demonstrate the performances of the MPBCD about the four different performance levels subjected to two hazard levels. A set of 20 ground motions listed within the SAC project is scaled to the DBE and MCE levels using the procedure by Somerville et al. (1997) to carry out nonlinear time-history analyses using these damper layouts and semi-active control designs. The details of scaling procedure and scale factors are available in Cha et al. (2014). As an example, the mean, median, and standard deviation of the maximum interstory drift for each of the nine-stories are calculated, as shown in Figure 2 for the PL1. The median plus standard deviation at the first story of the structure is slightly larger than the objective PLs under the DBE hazard level cases. The mean and median are within the objective PLs for the four design cases with significant reductions. The building's responses under the DBEs and MCEs calculated by the nonlinear time-history analyses appear to have met the performance levels for the nine-story building structure. For example, overall responses of each story are within linear elastic ranges that were predefined for each structural member by Ohtori et al. (2004), under the 21 DBEs for the PL1 0.7%. In addition, providing information concerning a wide range of efficient MR damper layouts with semi-active controller parameters, as shown in Tables 3 and 4, allows structural designers to effectively handle limitations placed on the installation of control devices because of architectural and mechanical system requirements.

8. CONCLUSION

Structural control devices have been widely developed and studied to reduce seismic responses for civil structures for more than three decades. However, the methodology for performance-based design integrated with structural control techniques has not been sufficiently studied. Traditional performance-based design methods with or without control systems have limitations in focusing on single performance levels under single hazard levels, which means that engineers and owners have limited design options due to budget amounts or structural or mechanical limitations. They also have to change section sizes or material properties, which is not applicable to existing structures. Hence, in this paper, a new performance-based control design methodology was proposed to provide various performance-based control design sets, satisfying multiple performance levels under multiple hazard levels simultaneously without changing member section sizes and material properties, by incorporating traditional performance-based design and controllers for use with MR dampers based on multi-objective optimization techniques. This numerical study used a DOFPC as a semi-active control algorithm, large-scale 200-kN MR dampers, a nine-story high-rise moment-resisting frame building, and GMGAs as a multi-objective genetic algorithm. The performance objectives were defined as minimizing the number of MR dampers in the MRF and minimizing the maximum interstory drift during nonlinear time-history analysis using single-design objective ground motion, thereby satisfying the maximum allowable interstory drifts at selected performance levels.

From the multi-objective optimization using a GMGA, multiple semi-active control designs and control device layouts for multiple performance levels were achieved simultaneously by parallel computing for multiple performance levels under multiple hazard levels. The achieved design sets significantly reduced the maximum drift of the example nine-story building with minimal control cost and best efficiency. The achieved performance-based design sets provide various design options to engineers and owners to freely select performance-based control designs by considering available budget amounts and structural or mechanical limitations for existing or newly constructing structures. The achieved designs were validated by nonlinear time-history analyses to evaluate the robustness about uncertainties of the hazard level by using with a suite of 20 earthquakes.

REFERENCES

Building Seismic Safety Council (BSSC). NEHRP recommended provisions for seismic regulations for new buildings and other structures. Rep. No. FEMA 450. Washington, D.C; 2003.

Cha, Y.-J., Agrawal, A. K., Kim, Y. and Raich, A. M. 2012. Multi-objective Genetic Algorithms for Cost-effective Distributions of Actuators and Sensors in Large Structures. *Expert Systems with Applications*, 39 (9): 7822-7833.

Cha, Y.-J. and Agrawal, A. K. 2013a. Velocity-based Semi-active Turbo-Lyapunov Control Algorithm for Seismically Excited Nonlinear Smart Structures. *Structural Control & Health Monitoring*, 20 (6): 1043-1056.

Cha, Y.-J. and Agrawal, A. K. 2013b. Decentralized Output Feedback Polynomial Control of Seismically Excited Structures Using Genetic algorithm. *Structural Control & Health Monitoring*, 20 (3): 241-258.

Cha, Y.-J., Kim, Y., Raich, A. M., and Agrawal, A. K. 2013a. Multi-objective Formulation for Actuator and Sensor Layouts of Actively Controlled 3-D Buildings. *Journal of Vibration and Control*, 19 (6): 942-960.

Cha, Y.-J., Raich, A. M., Barroso, L. R., and Agrawal, A. K. 2013b. Optimal Placement of Active Control Devices and Sensors in Frame Structures Using Multi-objective Genetic Algorithms. *Structural Control & Health Monitoring*, 20 (1): 16-44.

Cha, Y. J., Agrawal, A. K., Phillips, B. M., and Spencer, B. F. 2014. Direct performance-based design with 200kN MR dampers using multi-objective cost effective optimization for steel MRFs. *Engineering Structures*, *71*, 60-72.

Cha, Y. J., and Buyukozturk, O. 2015. Structural Damage Detection Using Modal Strain Energy and Hybrid Multiobjective Optimization. *Computer‐Aided Civil and Infrastructure Engineering*, 30(5): 347-358.

Deb, K., Agrawal, S., Pratab, A., and Meyarivan, T. 2000. A Fast Elitist Non-dominated Sorting Genetic Algorithm for Multi-objective Optimization: NSGA-II, KanGAL report 200001, Indian Institute of Technology, Kanpur, India.

Dyke, S. J., Spencer, B. F., Sain, M. K., and Carlson, J. D. 1996. Modeling and Control of Magnetorheological Dampers for Seismic Response Reduction. *Smart Materials and Structures*, 5: 565-575.

El-Khoury, O. and Adeli, H. 2013. Recent Advances on Vibration Control of Structures under Dynamic Loading. *Archives of Computational Methods in Engineering*, 20 (4): 353–360.

Federal Emergency Management Agency 2000a. Recommended Seismic Design Criteria for New Steel Moment-frame Buildings, Report No. FEMA-350, Washington, DC.

Federal Emergency Management Agency 2000b. Prestandard and Commentary for the Seismic Rehabilitation of Buildings, Report No. FEMA-356, Washington, DC.

Federal Emergency Management Agency 2003. NEHRP Recommended Provisions for Seismic Regulations for New Buildings and Other Structures, Building Seismic Safety Council, Report No. FEMA-450. Washington, D.C.

Fujitani, H., Teshigawara, M., Gojo, W., Hirano, Y., and Saito, T. 2005. Framework for Performance-based Design of Building Structures. *Computer‐Aided Civil and Infrastructure Engineering*, 20 (1): 62-77.

Ganzerli, S., Pantelides, C. P., and Reaveley, L. D. 2000. Performance-based Design Using Structural Optimization. *Earthquake Engineering and Structural Dynamics*, 29: 1677-1690.

Ghobarah, A. 2001. Performance-based Design in Earthquake Engineering: State of Development. *Engineering Structures*, 23: 878-884.

He, W. L., Agrawal, A. K., and Yang, J. N. 2003. A Novel Semi-active Friction Controller for Linear Structures Against Earthquakes. *Journal of Structural Engineering* ASCE, 129 (7): 941-950.

Hejazi, F., Toloue, I., Jaafar, M. S., and Noorzaei, J. 2013. Optimization of Earthquake Energy Dissipation System by Genetic Algorithm. *Computer‐Aided Civil and Infrastructure Engineering*, 28 (10): 796-810.

Kurata, N., Kobori, T., and Koshika, N. 2002. Performance-based Design With Semi-active Structural Control Technique. *Earthquake Engineering and Structural Dynamics*, 31: 445-458.

Lagaros, N. D., Fragiadakis, M., Papadrakakis, M., and Tsompanakis, Y. 2006. Structural Optimization: A Tool for Evaluating Seismic Design Procedures. *Engineering structures*, 28 (12): 1623-1633.

Lee, K. S., Ricles, J., and Sause, R. 2009. Performance-based Seismic Design of Steel MRFs with Elastomeric Eampers. *Journal of Structural Engineering*, 135 (5): 489-498.

Lee, K. S., Fan, C. P., Sause, R., and Ricles, J. 2005. Simplified Design Procedure for Frame Buildings with Viscoelastic and Elastomeric Structural Dampers. *Earthquake Eng. Struct. Dyn*., 34: 1271–1284.

MATLAB/SIMULINK. The Math Works: Natick, MA, 2007.

Moehle, J.P. 1992. Displacement-Based design of RC structures subjected to earthquakes. *Earthquake Spectra* 3 (4): 403-428.

Ohtori, Y., Christenson, R. E., Spencer, B. F. Jr., and Dyke, S. J. 2004. Benchmark Control Problems for Seismically Excited Nonlinear Buildings. *Journal of Engineering Mechanics*, 130 (4): 366-385.

Raich, A. M. and Ghaboussi, J. 2000. Evolving Structural Design Solution Using an Implicit Redundant Genetic Algorithm. *Structural Multidisciplinary Optimization*, 20: 222-231.

Somerville, P., Smith, N., Punyamurthula, S., and Sun, J. 1997. Development of Ground Motion Time Histories for Phase 2 of the FEMA/SAC Steel Project. Report No. SAC/BD-97/04, SAC Joint Venture, Sacramento, CA.

Spencer, B. F. Jr, Dyke, S. J., Sain, M. K., and Carlson, J. D. 1997. Phenomenological Model of a Magnetorheological Damper. *Journal of Engineering Mechanics*, ASCE, 123 (3): 230-238.

Yang, J. N., and Agrawal, A. K. 2002. Semi-active Hybrid Control Systems for Nonlinear Buildings Against Near-field Earthquakes. *Engineering Structures*, 24: 271-280.

Yang, J. N., Kim, J. H., and Agrawal, A. K. 2000. Resetting Semiactive Stiffness Damper for Seismic Response Control. *Journal of Structural Engineering*, ASCE 126 (12): 1427-1433.